

Original Paper

Growth of Endothelial Cells in Space and in Simulated Microgravity – a Comparison on the Secretory Level

Marcus Krüger^a Jessica Pietsch^a Johann Bauer^b Sascha Kopp^a
Daniel T. O. Carvalho^a Sarah Baatout^{c,d} Marjan Moreels^c Daniela Melnik^a
Markus Wehland^a Marcel Egli^e Jayashree Sahana^f Sara Dam Kobberø^f
Thomas J. Corydon^{f,g} Stefano Nebuloni^h Samuel Gass^h Matthias Evertⁱ
Manfred Infanger^a Daniela Grimm^{a,f}

^aClinic for Plastic, Aesthetic and Hand Surgery, Otto von Guericke University Magdeburg, Magdeburg, Germany, ^bMax Planck Institute of Biochemistry, Martinsried, Germany, ^cRadiobiology Unit, Belgian Nuclear Research Centre, Mol, Belgium, ^dMolecular Biotechnology, Ghent University, Ghent, Belgium, ^eInstitute of Medical Engineering, Space Biology Group, Lucerne University of Applied Sciences and Arts, Hergiswil, Switzerland, ^fDepartment of Biomedicine, Aarhus University, Aarhus, Denmark, ^gDepartment of Ophthalmology, Aarhus University Hospital, Aarhus, Denmark, ^hRUAG Slip Rings SA, Nyon, Switzerland, ⁱInstitute for Pathology, University of Regensburg, Regensburg, Germany

Key Words

Spaceflight • Microgravity • Cytokines • Extracellular matrix • Spheroids

Abstract

Background/Aims: Endothelial cells exposed to the Random Positioning Machine (RPM) reveal three different phenotypes. They grow as a two-dimensional monolayer and form three-dimensional (3D) structures such as spheroids and tubular constructs. As part of the ESA-SPHEROIDS project we want to understand how endothelial cells (ECs) react and adapt to long-term microgravity. **Methods:** During a spaceflight to the International Space Station (ISS) and a subsequent stay onboard, human ECs (EA.hy926 cell line) were cultured for 12 days in real microgravity inside an automatic flight hardware, specially designed for use in space. ECs were cultivated in the absence or presence of vascular endothelial growth factor, which had demonstrated a cell-protective effect on ECs exposed to an RPM simulating microgravity. After cell fixation in space and return of the samples, we examined cell morphology and analyzed supernatants by Multianalyte Profiling technology. **Results:** The fixed samples comprised 3D multicellular spheroids and tube-like structures in addition to monolayer cells, which are exclusively observed during growth under Earth gravity (1g). Within the 3D aggregates we detected enhanced collagen and laminin. The supernatant analysis unveiled alterations in secretion of several growth factors, cytokines, and extracellular matrix components as

compared to cells cultivated at 1g or on the RPM. This confirmed an influence of gravity on interacting key proteins and genes and demonstrated a flight hardware impact on the endothelial secretome. **Conclusion:** Since formation of tube-like aggregates was observed only on the RPM and during spaceflight, we conclude that microgravity may be the major cause for ECs' 3D aggregation.

© 2019 The Author(s). Published by
Cell Physiol Biochem Press GmbH&Co. KG

Introduction

Humans are adapted to the Earth's constant gravity, an important physical force significantly contributing to the normal function of our cardiovascular system. Astronauts returning from space have, among others, shown cardiovascular problems such as arrhythmias, cardiac atrophy, low blood pressure or orthostatic intolerance, accredited to endothelium injury [1-4]. Like other vascular cells, endothelial cells (ECs) are mechanoresponsive and react to physiological mechanical cues such as fluid shear stress, cyclic stretch, or hydrostatic pressure [5]. Therefore, it is not surprising that ECs are also sensitive to variations in gravity. During the last decade, several studies demonstrated significant modifications in ECs after exposure to altered gravity conditions [6-12]. It is assumed that they convert gravitational stimuli via gene regulation into biochemical signals [13]. Indeed, ECs showed alterations of secretory functions [14] as well as gravity-dependent modulation of EC processes, such as cellular proliferation, apoptosis, cytoskeletal organization, intracellular signaling mechanisms, and growth behavior [15-18]. Most interestingly, the exposure to microgravity (μg) generated a scaffold-free formation of three-dimensional (3D) cell aggregates called multicellular spheroids (MCS) [7, 19]. Small MCS with diameters of about 0.3 mm can be observed after a few days [20]. During an extended exposure, MCSs start to grow into tube-like structures reaching lengths of up to 2-3 mm [21]. Supplementation of vascular endothelial growth factor (VEGF) was shown to have cell-protective effects on ECs [8], but obviously does not affect the expression of adhesion molecules in MCS [22].

As the opportunities to perform long-term experiments on space crafts or space laboratories in real μg (r- μg) are rare due to high costs and a limited number of missions, most of the previous studies were conducted at 'ground-based facilities' such as the clinostat or the Random Positioning Machine (RPM), simulating some aspects of μg (simulated μg , s- μg). RPM-based studies showed that s- μg modifies the transcriptional [23] and translational [24] levels of gene expression in ECs. Recently, a long-term RPM experiment identified some key proteins involved in spheroid formation and angiogenesis [21].

Here, the ESA-SPHEROIDS project aimed to investigate the effects of r- μg on EC function, with respect to formation of blood vessel-like structures, cell proliferation, and apoptosis. Thus, the results of the SPHEROIDS project could help develop potential countermeasures to prevent cardiovascular deconditioning in astronauts and improve knowledge of endothelial function on Earth. For this purpose, we performed an experiment onboard the International Space Station (ISS) in 2016 to observe human ECs remaining in space for 5 d and 12 d [25] in order to increase our knowledge in the behavior of human ECs exposed to r- μg . The objective of this study was three-fold. First, we focused on the growth behavior of cells treated without or with vascular endothelial growth factor (VEGF) in space. Second, we studied the secretion behavior of ECs applying MAP technology and third, we performed an RPM experiment exactly copying the time and temperature protocols of the ISS mission and compared these results with the data received from the space samples. After completion of the experiments we analyzed the release of cytokines and extracellular matrix (ECM) proteins involved in 3D growth and cell adhesion such as laminin and fibronectin.

Materials and Methods

Cell culture

We used the permanent human cell line EA.hy926 (CRL-2922; ATCC, Manassas, VA, USA), which had been established by fusing human umbilical vein endothelial cells (HUVECs) with the permanent cell line A549, derived from a human lung carcinoma. Although a hybrid, EA.hy926 cells still exhibit characteristic EC features [26, 27]. The cells were cultivated in RPMI-1640 medium (Invitrogen, Eggenstein, Germany) containing 100 μ M sodium pyruvate and 2 μ M L-glutamine (Thermo Fisher Scientific, Waltham, MA, USA) and 10% Fetal Calf Serum (FCS), 100 U/mL penicillin and 100 μ g/mL streptomycin (all Biochrom, Berlin, Germany).

The cells were maintained in 75-cm² tissue culture flasks (Sarstedt, Nümbrecht, Germany) until monolayers were formed, reaching a confluency of approximately 80%. One day prior to the experiments, the EA.hy926 cells were suspended in RPMI-1640 medium so that the cells could be seeded in cultivation chambers (RUAG Space, Nyon, Switzerland) or in slide flasks (Nunc™ Lab-Tek™ SlideFlask; Thermo Fisher Scientific) for a preliminary 24 h-period of adherence. In this stage the cultures were used in the different experimental scenarios.

Flight hardware

The flight hardware was designed, developed and manufactured by RUAG Space (Nyon, Switzerland). SPHEROIDS received 8 experimental units each containing two independent cultivation chambers (CC) with adhesion surfaces made of polyether ether ketone (PEEK). Materials were intensely tested for biocompatibility [25]. For each experimental unit, one CC was filled with RPMI-1640 medium, the other one was filled with RPMI-1640 supplemented with 10 μ g/mL VEGF-A (Sigma-Aldrich, Deisenhofen, Germany; further referred as VEGF). The assembly procedure preceding the spaceflight and the cell harvest after the mission has been previously described by Pietsch and coworkers [25]. 5×10^5 and 4×10^5 cells were seeded in the cultivation chambers for the 7-day experiment or the 14-day experiment respectively before handover to NASA. A timeline for automatic medium exchange and fixation had to be programmed prior to the spaceflight. Therefore, all worst-case scenarios (launch scrubs, delays until berthing at the ISS, until installation in KUBIK, and until turning-on power supply) had to be considered. Ultimately, we collected μ g-phases of 5 d and 12 d in our experiments. If a delay had occurred, it could have been longer. If all delays occurred, we would have got the maximum of 7 d and 14 d of r- μ g.

Dragon spaceflight with SpaceX CRS-8

SpaceX CRS-8 was a commercial resupply service mission transporting a total cargo load of over 3,100 kg to the ISS, including multiple experiments. On April 8th, 2016 at 20:43 UTC SPHEROIDS was launched in a Dragon capsule on board SpaceX CRS-8 from NASA's Kennedy Space Center in Florida. After 41 h and 14 min Dragon was berthed at the ISS. After completion of the mission, the flight hardware returned to Earth on May 11th, 2016 and was subsequently shipped to our laboratories.

Time and temperature were logged continuously via temperature sensing iButtons (iButtonLink, Whitewater, WI, USA; accuracy $\pm 0.5^\circ\text{C}$) on top of the experimental units. The protocols for both, the 7-day and the 14-day experiments are shown in Fig. 1. The same protocols were subsequently used for the ground control and the RPM experiment.

Random Positioning Machine (RPM)

The RPM was developed as a '3D clinostat' to simulate μ g [28]. Our device was manufactured by Airbus Defence and Space and is used routinely in our laboratory. Cell culture experiments on the RPM had been investigated thoroughly and previously published in detail [18, 20, 29-32]. For the SPHEROIDS RPM experiment 10^6 cells were seeded in slide flasks ($n = 5/\text{group}$). After sub-confluent monolayers had formed, the slide flasks were filled completely with medium (air bubble-free), subsequently positioned on the inner frame of the RPM and the rotation was started at a speed of $60^\circ/\text{s}$ using real random mode (random speed and random direction) according to the spaceflight timescale. For the experiment, the RPM was positioned in a standard incubator using the spaceflight temperature protocol (Fig. 1). In parallel, slide flasks were placed next to the RPM in the incubator as $1g$ -controls ($n = 5/\text{group}$).

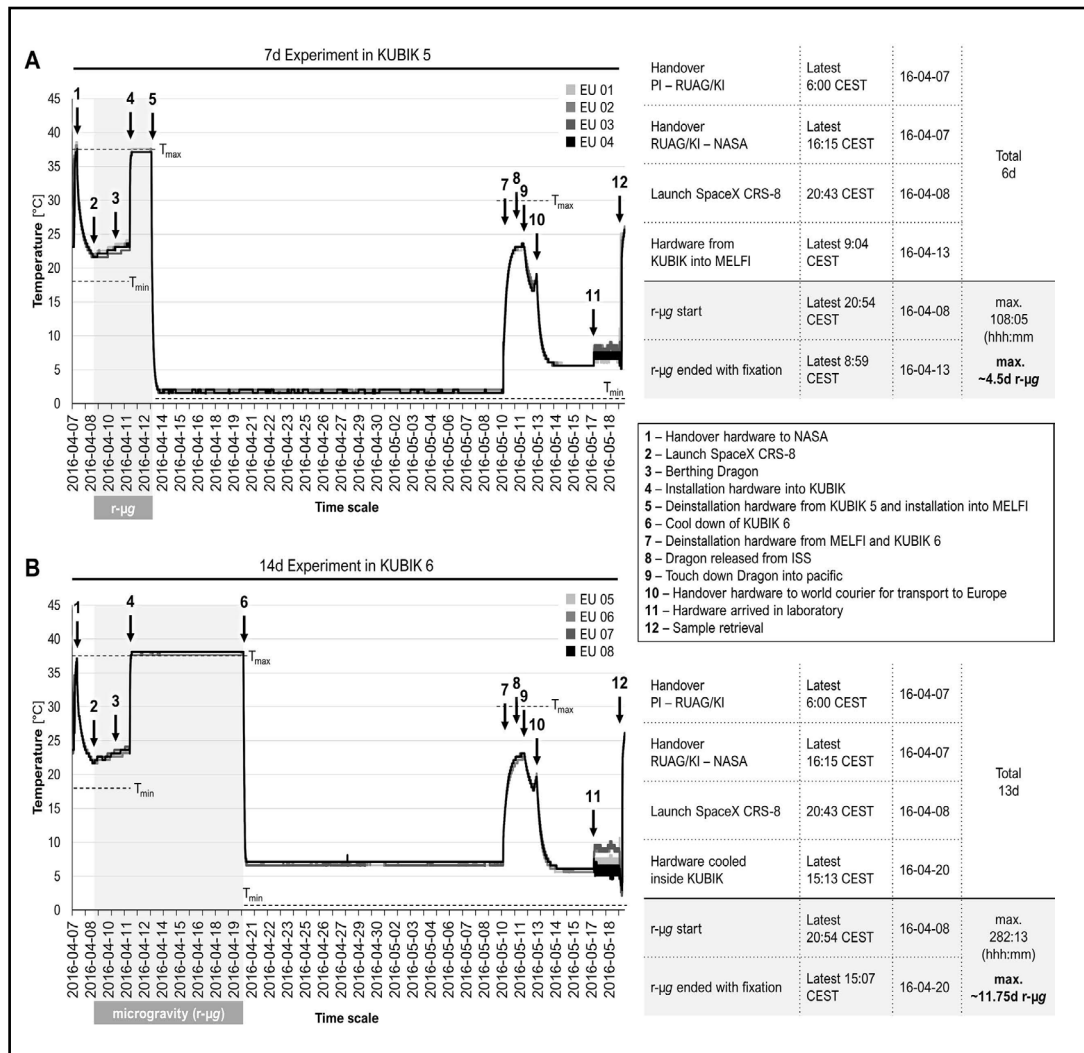


Fig. 1. Temperature profiles of the complete mission starting from shortly before handover of the flight hardware until the retrieval of the samples. Temperature was logged by thermosensors every 10 min on the top of every experimental unit. A) Four units were installed in KUBIK 5 for the 7-day experiment. B) Another four units were installed in KUBIK 6 for the 14-day experiment. The phase when living cells were exposed to r-μg is drawn in grey. It ended with fixation. Dashed lines at 37.5°C and 0.5°C represent the maximum and minimal required temperature, respectively. EU: Experimental unit.

Morphology and cytochemistry

We used the hematoxylin/eosin (HE) staining method, which has been described earlier in detail [25, 33]. Multicellular spheroids and tubular structures had been PFA-fixed in space. They were paraffin-embedded, sectioned and mounted on object slides, deparaffinized and after rehydration stained with HE or Sirius red. All sections were visualized by light microscopy using a LEICA DM2000 microscope equipped with a Leica DFC310 FX digital CCD color camera.

Immunofluorescence microscopy (IFM)

To visualize laminin, the slides were incubated using a laminin-specific primary antibody (Sigma-Aldrich) followed by a peroxidase-labeled secondary antibody. Antigen-antibody complexes were visualized by the indirect immunoperoxidase technique [34].

Cytokine measurements by Multianalyte Profiling (MAP) technology

The altered cytokines and proteins released into the cell culture supernatants were analyzed by the company Myriad RBM (Austin, TX, USA). The MAP analysis was performed using the Human InflammationMAP® as described previously [35]. Supernatants were collected from 1g- and µg-samples after the 7 d and 14 d timepoints (flight hardware: n = 4, slide flasks: n = 5) and stored at -80°C prior to the analysis at Myriad RBM.

Collagen type I, laminin and fibronectin measurements from cell culture supernatants

Protein levels were determined using a commercial ELISA kits according to the manufacturer's instructions (LifeSpan BioSciences, Seattle, WA, USA; Cusabio Biotech, Houston, TX, USA). Supernatant samples harvested from the flight hardware were used undiluted. Supernatants of the cell culture flasks were diluted 1:1 (laminin, collagen type I 1g) or 1:10 (fibronectin, collagen type I RPM). 96-well plates were read using a SpectraMax M2 Microplate Reader (Molecular Devices, San José, CA, USA). Data was analyzed via elisaanalysis.com (Elisakit.com, Melbourne, Australia) with a 4-parameter logistic regression algorithm for standard curve equation.

RNA isolation and quantitative real-time PCR

RNA isolation and quantitative real-time PCR (qPCR) were performed as described earlier in detail [25, 36, 37]. ECs had been fixed with RNAlater® (Sigma-Aldrich) at the end point of the experiments. RNA and protein were isolated using the RNeasy® Kit (Qiagen, Hilden, Germany) according to the manufacturer's recommendations. Concentrations were determined via optical density at 260 and 280 nm with a NanoDrop™ 2000 (Thermo Fisher Scientific, Waltham, MA, USA). Complementary DNA (cDNA) was produced using the First Strand cDNA Synthesis Kit (Thermo Fisher Scientific) following manufacturer's instructions. The expression levels of the following target genes were determined via qPCR: *B2M*, *CCL2*, *CCL11*, *CDH5*, *COL1A1*, *CXCL8*, *FN1*, *FTL*, *IL6*, *LAMA1*, *LAMB2*, *TIMP1*, *VEGFA*, and *18S*, using the SYBR® Select Master Mix (Applied Biosystems, Darmstadt, Germany) and the 7500 Fast Real-Time PCR System (Applied Biosystems). cDNA-selective primers were designed to span exon-exon boundaries and to have a T_m of 60°C using Primer Express software (Applied Biosystems), and were synthesized by TIB Molbiol (Berlin, Germany). The sequences of the forward and reverse primers are listed in Table 1. All samples were measured in triplicate and normalized against 18S rRNA as a housekeeping gene. Comparative C_t (ΔΔC_t) methods were used for relative quantification of transcription levels, with 1g set as 100%.

Pathway analysis

To investigate and visualize interactions between selected proteins and genes, we input relevant UniProtKB entry numbers into the Pathway Studio v.11 software (Elsevier Research Solutions, Amsterdam, the Netherlands). The identified genes were analyzed according to their mutual regulation. The proteins were evaluated in regard to their cellular localization and their interaction.

Table 1. Primers used for qPCR

Gene	Primer	Sequence (5'-3' direction)
<i>18S</i>	18S-F	GGAGCCTGCGGCTTAATTT
	18S-R	CAACTAAGAACGGCCATGCA
<i>B2M</i>	B2M-F	CACTGAATTACCCCCACTGA
	B2M-R	GCTTACATGTCTCGATCCCAC
<i>CCL2</i>	MCP1-F	GCTATAGAAGAATCACCAGCAGCAA
	MCP1-R	TGGAATCCTGAACCCACTTCTG
<i>CCL11</i>	CCL11-F	CCAACCCTGTGCTTTAAC
	CCL11-R	GTCTTGAAGATCACAGCTTTCTG
<i>CDH5</i>	CDH5-F	GTCTGCAGATCTCCGCAAT
	CDH5-R	TGTTGGCCGTGTTATCGTGA
<i>COL1A1</i>	COL1A1-F	ACGAAGACATCCCACCAATCAC
	COL1A1-R	CGTTGTCGACAGCGCAGAT
<i>CXCL8</i>	IL8-F	TGGCAGCCTTCTGATTTCT
	IL8-R	GGGTGAAAGGTTTGGAGTATG
<i>FTL</i>	FTL-F	CTTGCCAACCAACCATGAGC
	FTL-R	AGAAGCCCAGAGAGAGGTAGG
<i>IL6</i>	IL6-F	CGGGAACGAAAGAGAAGCTCTA
	IL6-R	GAGCAGCCCCAGGGAGAA
<i>FN1</i>	FN1-F	TGAGGAGCATGGTTTTAGGAGAA
	FN1-R	TCCTCATTTACATTCGGCGTATAC
<i>LAMA1</i>	LAMA1-F	TGACTGACCTGGGTTTCAGGA
	LAMA1-R	TGCTAGACTCCTTGCTTCC
<i>LAMB2</i>	LAMB2-F	TGCTCATGGTCAATGCTAATCTG
	LAMB2-R	TCTATCAATCCTTCTTGGACAA
<i>TIMP1</i>	TIMP1-F	GCCATCGCCGAGATC
	TIMP1-R	GCTATCAGCCACAGCAACAACA
<i>VEGFA</i>	VEGFA-F	GCGCTGATAGACATCCATGAAC
	VEGFA-R	GCGCTGATAGACATCCATGAAC

Statistical Evaluation

The statistical evaluation was performed using SPSS 15.0 (SPSS Inc., Chicago, IL, USA). The Mann-Whitney-U-Test was used to compare $1g$ and μg conditions, 7 d and 14 d samples, samples with/without supplemented VEGF, as well as AD cells and MCS cells. All data is presented as mean \pm standard deviation (SD) with a significance level of $p < 0.05$.

Results

The SPHEROIDS experiment

After all materials had been extensively tested for biocompatibility in our laboratory [25], a novel and enhanced flight hardware was available for the space experiment in early 2016. It consisted of eight experimental units, each containing two cell culture chambers, two separate medium chambers, two supernatant chambers, and one fixation chamber. The medium compartments (Fig. 2A) were filled with culture medium (Fig. 2B), the fixation compartments (Fig. 2C) with fixation fluid (half of the units with PFA for investigation of cell structures and cytochemistry, the other half with RNA*later* for transcriptional analyses; Fig. 2D). Next, the compartments were assembled (Fig. 2E) and connected with the cell culture chamber via pumps for automatic medium exchange and cell fixation (Fig. 2F, G). Last, two cell cultivation chambers (Fig. 2H, CC (E1) and CC (E2)) were added on top of the experimental unit (Fig. 2G) and filled with cells and medium. In each experimental unit, one cell cultivation chamber was filled with cells suspended in plain medium, the other one was filled with cells suspended in medium supplemented with VEGF ($c = 10 \mu g/mL$). During the space experiment four experimental units were incubated for a 7 d timeframe, the remaining four for the length of 14 d.

Two days before the launch on April 8th, the entire flight hardware was handed over to the NASA engineers, who placed it into the rocket at a temperature of 22°C. 10 minutes after launch the cells had already entered microgravity. After a two-day flight to the ISS at 22-23°C, astronauts placed the hardware inside the KUBIK incubator facility [38] in the European Columbus Laboratory (Fig. 3A). The cells continued proliferating under $r\text{-}\mu g$ conditions. Cells of four experimental units were automatically chemically fixed on the day 7 after handover (7 d samples \approx 5 d in $r\text{-}\mu g$). A medium exchange was executed on the remaining 4 experimental units. Then the cells were allowed to proliferate on the ISS for another seven days before fixation (14 d samples \approx 12 d in $r\text{-}\mu g$). Afterwards, the fixed EA.hy926 cells were stored at 4°C and remained in space, before returning to Earth on May 11th for subsequent analysis in the home laboratory (Fig. 3B). The flight hardware was cleaned, refilled and used for the ground control experiments, repeating the exact spaceflight protocol under normal $1g$ conditions (ground control; Fig. 3A). Furthermore, to study the effects of $s\text{-}\mu g$ in the laboratory, an additional experiment was performed on an RPM. Slide flasks offering a similar growth area and volume as the cultivation chambers (CCs) used as flight hardware, but could be installed on a desktop RPM were used for this additional experiment. The ground control as well as the RPM experiments were performed copying the exact time and temperature protocols of the space experiment (Fig. 1).

Growth behavior of EA.hy926 cells in microgravity

When cells returned from space, we were able to harvest the three different types of EA.hy926 cells. One part of the ECs stayed adherent (AD) over the course of 7 and 14 days (Fig. 3C). In addition, we recognized a scaffold-free formation of different 3D aggregates. Some of the formations were 3D structures with spherical appearance, called multicellular spheroids (MCS) (Fig. 3D), others were detected as tube-like structures (Fig. 3E, F). This demonstrates that ECs exhibit 3D growth in space similarly to their growth on the RPM (Fig. 3G).

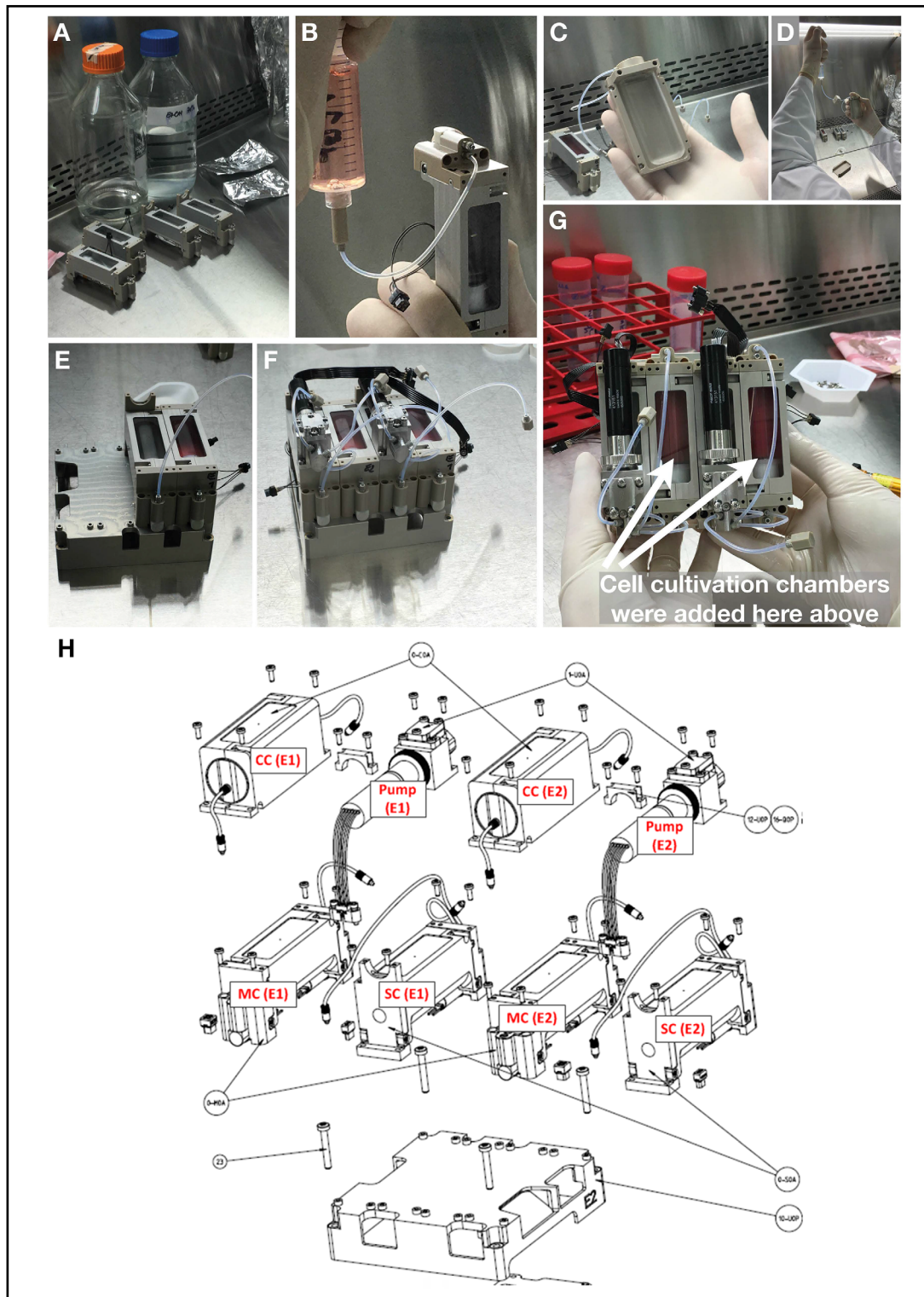


Fig. 2. Assembly and preparation of the SPHEROIDS flight hardware. A, B) The medium chambers were filled with cell culture medium. C, D) The fixation chamber was filled with fixation fluid, PFA or RNAlater. E, F) Medium chambers and supernatant chambers were assembled. G) The experimental unit before adding the cultivation chambers. H) Assembly of modules onto main support. The dimensions of one assembled hardware unit are 10 × 10 × 10 cm. CC: Cultivation chamber, E1: Experiment 1 (-VEGF), E2: Experiment 2 (+VEGF), MC: Medium chamber, SC: Supernatant chamber.

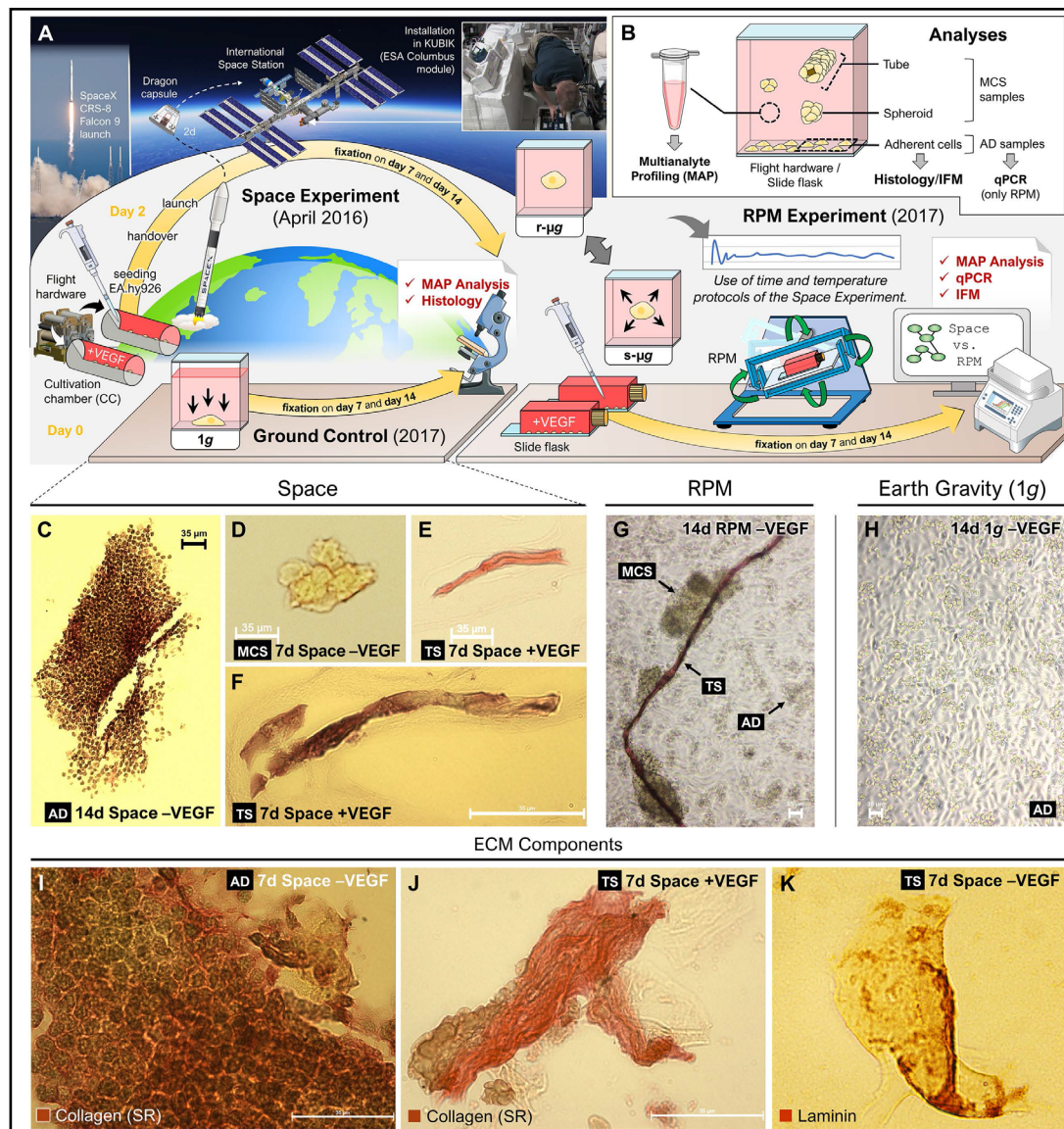


Fig. 3. Overview of the SPHEROIDS experiments. A) The SPHEROIDS study consisted of a space experiment that was conducted for two weeks on the ISS, a ground control, and an additional RPM experiment. B) Set of analyses that were done after the experiments. C-F) Morphology of space-grown EA.hy926 cells harvested from the flight hardware: Adherent cells (AD) after 14 d (C), multicellular spheroids (MCS) (D) and tube-like structures (TS) after 7 d (E,F). G) Morphology of EA.hy926 cells cultured for 12 d on the RPM and (H) under 1g conditions. I) Adherently growing EA.hy926 cells after 5 d in space. J) A multicellular tube harvested from the 7-day space samples. ECs were stained with Sirius Red (showing collagen in red). K) Laminin staining of a tubular structure, grown for 5 d in space. Scale bars: 35 μm. Parts of the Fig. were drawn by using pictures from Servier Medical Art. Servier Medical Art by Servier is licensed under a Creative Commons Attribution 3.0 Unported License (<https://creativecommons.org/licenses/by/3.0/>).

The ECs stayed viable during the spaceflight and continued to produce ECM components. Collagen production occurred in AD cells and in 3D aggregates. This was visualized by Sirius red staining of paraffin-embedded ECs, collected from the flight hardware after the spaceflight (Fig. 3I, J). Laminin was also found occluded in the 3D structures (Fig. 3K).

Table 2. Extracellular matrix proteins released by EA.hy926 cells after space-exposure compared with 1g controls. The cells were cultured in CCs of the flight hardware. The data was generated by using ELISA. Values are given as mean ± SD; LLOQ: Lower Limit of Quantitation, lowest concentration of an analyte in a sample that can be reliably detected

Factor	Earth gravity (1g)				Space (ISS mission)				LLOQ	Unit
	7 d		14 d		7 d		14 d			
	- VEGF	+ VEGF	- VEGF	+ VEGF	- VEGF	+ VEGF	- VEGF	+ VEGF		
Fibronectin	4.734 ± 0.095	4.847 ± 0.328	5.463 ± 0.638	4.951 ± 0.538	5.218 ± 1.469	5.126 ± 1.939	5.027 ± 0.167	5.205 ± 0.307	0.156	ng/mL
Laminin A / Laminin B	0.371 ± 0.058	0.342 ± 0.185	0.314 ± 0.187	0.187 ± 0.130	0.676 ± 0.423	0.764 ± 0.386	0.465 ± 0.036	0.434 ± 0.078	0.156	ng/mL
Collagen Type I	0.350 ± 0.582	<1.560	0.990 ± 0.868	0.003 ± 0.006	11.67 ± 5.74	15.70 ± 13.23	4.776 ± 0.240	4.649 ± 2.264	1.560	ng/mL

Table 3. Extracellular matrix proteins released by EA.hy926 cells after exposure to the RPM compared with 1g controls. Cells were cultured in slide flasks. The data was generated by using ELISA. Values are given as mean ± SD; *: P < 0.05 vs. 1g; ▼|▲: P < 0.05 vs. 7d; §: P < 0.05 vs. -VEGF; LLOQ: Lower Limit of Quantitation, lowest concentration of an analyte in a sample that can be reliably detected

Factor	Earth gravity (1g)				RPM (s-μg)				LLOQ	Unit
	7 d		14 d		7 d		14 d			
	- VEGF	+ VEGF	- VEGF	+ VEGF	- VEGF	+ VEGF	- VEGF	+ VEGF		
Fibronectin	23.31 ± 2.52	21.21 ± 1.80	23.69 ± 1.76	▲27.12 ± 4.04	22.37 ± 1.74	22.42 ± 1.90	26.19 ± 4.24	24.44 ± 2.20	0.156	ng/mL
Laminin A / Laminin B	7.079 ± 0.723	7.629 ± 1.086	▲13.34 ± 1.41	▲11.54 ± 1.10	9.92* ± 1.361	9.321 ± 1.139	12.05 ± 1.11	10.42 ± 1.07	0.156	ng/mL
Collagen Type I	6.686 ± 1.197	7.277 ± 1.235	▲28.85 ± 2.73	▲23.57§ ± 1.41	16.64 ± 8.42	14.62 ± 7.97	▲34.68 ± 12.80	▲39.07* ± 14.89	1.560	ng/mL

Release of extracellular matrix components

As shown above, collagen was secreted and incorporated into the ECM. In addition, together with several growth factors and cytokines, collagen and some other components of the ECM were released into the supernatant. Using MAP technology and ELISA, a number of proteins released into the supernatant under microgravity and control conditions were quantified (Tables 2-5).

Tables 2 and 3 indicate that much more fibronectin and laminin were produced, when the ECs were incubated in normal polystyrene slide flasks than during incubation in the newly developed CC suitable for culturing cells in space. This was true, even if the flasks or chambers were incubated under normal laboratory conditions according to equal protocols. However, under laboratory conditions, much more collagen I was secreted in slide flasks than in CCs. Though, similar amounts of collagen were found when the cells had been incubated under simulated or real microgravity independent of the material of the culture dish.

Release of matrix regulators, growth factors and cytokines

When the Human InflammationMAP® was applied to search for cellular proteins released into the supernatant, only part of the antibodies deployed indicated the presence of their targets (Tables 4, 5). In addition, the detection of specific proteins in the supernatant depended on the type of culture dish, wherein the cells were suspended. Differences of secretion, which depended on the type of culture dish were also found when the growth

Table 4. Proteins released by EA.hy926 cells after space-exposure compared with 1g controls. The cells were cultured in CCs of the flight hardware. The data was generated by Multi-Analyte Profiling using the Myriad RBM Human Inflammation MAP® v1.0. Values are given as mean ± SD; *: P <0.05 vs. 1g; ▼|▲: P <0.05 vs. 7d; §: P <0.05 vs. -VEGF; LLOQ: Lower Limit of Quantitation, lowest concentration of an analyte in a sample that can be reliably detected. The values are determined as the mean of 5 (1g control) or 13 (RPM) blank readings. C-Reactive Protein (CRP), Factor VII, Granulocyte-Macrophage Colony-Stimulating Factor (GM-CSF), Haptoglobin, Intercellular Adhesion Molecule 1 (ICAM-1), Interferon γ (IFN-γ), Interleukin-1 beta (IL-1β), Interleukin-1 receptor antagonist (IL-1ra), Interleukin-2 (IL-2), Interleukin-3 (IL-3), Interleukin-4 (IL-4), Interleukin-5 (IL-5), Interleukin-7 (IL-7), Interleukin-10 (IL-10), Interleukin-12 Subunit p70 (IL-12p70), Interleukin-15 (IL-15), Interleukin-17 (IL-17), Interleukin-18 (IL-18), Interleukin-23 (IL-23), Macrophage Inflammatory Protein-1α (MIP-1α), Macrophage Inflammatory Protein-1β (MIP-1β), Matrix Metalloproteinase-3 (MMP-3), Matrix Metalloproteinase-9 (MMP-9), Stem Cell Factor (SCF), T-Cell-Specific Protein RANTES (RANTES), Tumor Necrosis Factor α (TNF-α), Tumor Necrosis Factor β (TNF-β), Tumor Necrosis Factor Receptor 2 (TNFR2), Vascular Cell Adhesion Molecule-1 (VCAM-1), Vitamin D-Binding Protein (VDBP), and von Willebrand Factor (vWF) levels were below the LLOQ

Factor	Earth gravity (1g)				Space (ISS mission)				LLOQ	Unit
	7 d		14 d		7 d		14 d			
	- VEGF	+ VEGF	- VEGF	+ VEGF	- VEGF	+ VEGF	- VEGF	+ VEGF		
α1-Antitrypsin (AAT)	<0.075	<0.075	<0.075	0.183 ± 0.365	<0.075	<0.075	<0.075	<0.075	0.075	ng/mL
α2-Macroglobulin (A2M)	1.225 ± 0.150	1.150 ± 0.058	1.148 ± 0.196	1.125 ± 0.050	1.055 ± 0.090	1.250 ± 0.191	1.350 ± 0.071	1.400 ± 0.141	0.520	µg/mL
β2-Microglobulin (β2M)	1.455 ± 0.369	1.825 ± 0.512	▼0.417 ± 0.237	▼0.093 ± 0.027	2.100* ± 0.283	2.025 ± 0.776	0.705 ± 0.021	0.730 ± 0.014	0.042	ng/mL
Brain-Derived Neurotrophic Factor (BDNF)	<0.008	<0.008	<0.008	<0.008	0.010 ± 0.012	0.012 ± 0.014	<0.008	<0.008	0.008	ng/mL
Complement C3 (C3)	<0.027	<0.027	<0.027	0.126 ± 0.224	<0.027	<0.027	<0.027	<0.027	0.027	ng/mL
Eotaxin-1	9.50 ± 10.96	5.75 ± 11.50	<16	▲38.50§ ± 8.19	<16	<16	<16	<16	16	pg/mL
Ferritin (FRTN)	0.151 ± 0.066	0.170 ± 0.058	▼0.028 ± 0.019	▼<0.034	0.185 ± 0.040	0.129 ± 0.069	0.039 ± 0.004	0.047 ± 0.002	0.034	ng/mL
Fibrinogen	<0.065	<0.065	<0.065	0.788 ± 1.413	<0.065	<0.065	<0.065	<0.065	0.065	ng/mL
Interleukin-1α (IL-1 alpha)	0.165 ± 0.195	0.185 ± 0.226	0.080 ± 0.160	0.368§ ± 0.015	0.155 ± 0.186	0.175 ± 0.206	<0.280	0.280	0.280	pg/mL
Interleukin-6 (IL-6)	1.650 ± 0.443	1.950 ± 0.985	▼<0.580	▼<0.580	4.150 ± 2.829	4.400 ± 4.311	0.700 ± 0.990	1.700 ± 0.000	0.580	pg/mL
Interleukin-8 (IL-8)	80.25 ± 22.94	90.75 ± 25.62	▼18.23 ± 9.65	▼8.58 ± 3.95	104.25 ± 103.1	113.13 ± 120.4	66.50 ± 9.19	59.00 ± 5.66	1.600	pg/mL
Interleukin-12 Subunit p40	0.066 ± 0.047	0.068 ± 0.057	0.067 ± 0.047	0.156 ± 0.071	<0.047	<0.047	<0.047	<0.047	0.047	ng/mL
Monocyte Chemotactic Protein 1 (MCP-1)	0.241 ± 0.062	0.279 ± 0.083	▼0.025 ± 0.017	▼<0.022	0.154 ± 0.033	0.169 ± 0.066	0.034 ± 0.007	0.029 ± 0.014	0.022	ng/mL
Tissue Inhibitor of Metalloproteinases 1 (TIMP-1)	1.095 ± 0.342	1.323 ± 0.407	0.507 ± 0.306	▼0.096 ± 0.034	0.825 ± 0.318	0.765 ± 0.448	0.255 ± 0.007	0.280 ± 0.014	0.013	ng/mL
Vascular Endothelial Growth Factor (VEGF)	15.8 ± 2.1	1883 ± 229	19.1 ± 9.8	▲7905 ± 679	<8.8	824 ± 686	<8.8	1430 ± 99	8.8	pg/mL

Table 5. Proteins released by EA.hy926 cells after exposure to the RPM compared with 1g controls. The cells were cultured in slide flasks. The data was generated by Multi-Analyte Profiling using the Myriad RBM Human Inflammation MAP® v1.0. Values are given as mean ± SD, *: P <0.05 vs. 1g; ▼|▲: P <0.05 vs. 7d; §: P <0.05 vs. -VEGF; LLOQ: Lower Limit of Quantitation, lowest concentration of an analyte in a sample that can be reliably detected. The values are determined as the mean of 5 (1g control) or 13 (RPM) blank readings. C-Reactive Protein (CRP), Factor VII, Fibrinogen, Granulocyte-Macrophage Colony-Stimulating Factor (GM-CSF), Haptoglobin, Interferon γ (IFN-γ), Interleukin-1β (IL-1β), Interleukin-1 receptor antagonist (IL-1ra), Interleukin-2 (IL-2), Interleukin-3 (IL-3), Interleukin-4 (IL-4), Interleukin-5 (IL-5), Interleukin-7 (IL-7), Interleukin-10 (IL-10), Interleukin-12 Subunit p40 (IL-12p40), Interleukin-12 Subunit p70 (IL-12p70), Interleukin-15 (IL-15), Interleukin-17 (IL-17), Interleukin-18 (IL-18), Interleukin-23 (IL-23), Macrophage Inflammatory Protein-1α (MIP-1α), Macrophage Inflammatory Protein-1β (MIP-1β), Matrix Metalloproteinase-9 (MMP-9), Stem Cell Factor (SCF), Tumor Necrosis Factor alpha (TNF-α), Tumor Necrosis Factor β (TNF-β), Vascular Cell Adhesion Molecule-1 (VCAM-1), and Vitamin D-Binding Protein (VDBP) levels were below the LLOQ

Factor	Earth gravity (1g)				RPM (s-μg)				LLOQ	Unit
	7 d		14 d		7 d		14 d			
	- VEGF	+ VEGF	- VEGF	+ VEGF	- VEGF	+ VEGF	- VEGF	+ VEGF		
α1-Antitrypsin (AAT)	<0.075	<0.075	▲0.205 ± 0.017	▲0.178 ± 0.019	<0.075	0.017 ± 0.038	▲0.248 ± 0.066	▲0.272* ± 0.041	0.075	ng/mL
α2-Macroglobulin (A2M)	1.113 ± 0.118	0.965 ± 0.052	1.175 ± 0.171	0.965 ± 0.090	0.974 ± 0.021	1.018 ± 0.078	1.015 ± 0.103	1.102 ± 0.136	0.520	μg/mL
β2-Microglobulin (B2M)	18.75 ± 5.44	18.75 ± 4.65	▲75.25 ± 6.34	▲73.75 ± 4.27	23.40 ± 8.20	24.80 ± 6.34	▲74.25 ± 12.09	▲85.60 ± 15.71	0.042	ng/mL
Brain-Derived Neurotrophic Factor (BDNF)	0.140 ± 0.027	0.103 ± 0.039	0.260 ± 0.174	▲0.378 ± 0.082	0.170 ± 0.040	0.156 ± 0.041	▲0.418 ± 0.123	▲0.506 ± 0.103	0.008	ng/mL
Complement C3 (C3)	<0.027	<0.027	▲0.173 ± 0.021	▲0.193 ± 0.021	0.012 ± 0.036	0.029 ± 0.033	▲0.203 ± 0.039	▲0.200 ± 0.080	0.027	ng/mL
Eotaxin-1	4.50 ± 9.00	27.75§ ± 3.40	4.50 ± 9.00	20.25 ± 3.30	7.20 ± 9.86	28.40§ ± 4.16	<16	31.60§ ± 6.84	16	pg/mL
Ferritin (FRTN)	0.140 ± 0.020	0.165 ± 0.013	▲0.343 ± 0.106	▲0.303 ± 0.026	0.228* ± 0.102	0.252* ± 0.052	▲0.508 ± 0.078	▲0.594§ ± 0.096	0.034	ng/mL
Intercellular Adhesion Molecule 1 (ICAM-1)	<0.570	<0.570	0.455 ± 0.308	▲0.640 ± 0.052	0.114 ± 0.255	0.114 ± 0.255	0.455 ± 0.308	▲0.822* ± 0.120	0.570	ng/mL
Interleukin-1α (IL-1 alpha)	<0.280	<0.280	0.090 ± 0.180	0.170 ± 0.197	0.064 ± 0.143	0.296 ± 0.173	▲0.585* ± 0.163	▲0.726* ± 0.138	0.280	pg/mL
Interleukin-6 (IL-6)	5.90 ± 0.54	5.60 ± 1.47	▲35.00 ± 1.41	▲38.25 ± 4.92	18.24* ± 16.13	18.40* ± 7.83	▲157.0* ± 44.80	▲185.0* ± 77.39	0.580	pg/mL
Interleukin-8 (IL-8)	50.25 ± 10.59	43.25 ± 11.18	▲192.0 ± 18.67	▲192.0 ± 25.74	93.20* ± 28.26	97.60* ± 22.07	▲297.3* ± 65.07	▲322.4* ± 97.82	1.600	pg/mL
Matrix Metalloproteinase-3 (MMP-3)	<0.010	<0.010	0.003 ± 0.006	0.004 ± 0.008	<0.010	0.002 ± 0.005	▲0.021* ± 0.006	▲0.031* ± 0.010	0.010	ng/mL
Monocyte Chemotactic Protein 1 (MCP-1)	3.06 ± 1.43	3.84 ± 0.40	▲9.72 ± 1.60	▲10.99 ± 1.02	6.97* ± 1.71	6.03* ± 1.25	▲19.88* ± 4.72	▲24.78* ± 5.81	0.022	ng/mL
T-Cell-Specific Protein RANTES (RANTES)	14.00 ± 2.94	11.60 ± 2.33	▲38.75 ± 3.10	▲38.50 ± 2.65	23.00* ± 4.06	22.80* ± 2.49	▲67.00 ± 24.93	▲76.40* ± 22.15	1.1	pg/mL
Tissue Inhibitor of Metalloproteinases 1 (TIMP-1)	23.25 ± 10.05	27.00 ± 6.32	▲77.00 ± 5.48	▲69.75 ± 8.22	29.80 ± 8.93	33.00 ± 9.27	▲66.50 ± 8.27	▲71.40 ± 23.84	0.013	ng/mL
Tumor Necrosis Factor Receptor 2 (TNFR2)	2.50 ± 5.00	7.75 ± 5.19	▲18.75 ± 5.56	▲18.50 ± 1.91	20.40* ± 15.65	28.20* ± 10.99	26.25 ± 7.41	18.20 ± 6.87	10	pg/mL
Vascular Endothelial Growth Factor (VEGF)	<8.8	3990 ± 1234	▲17.0 ± 2.8	▼1998 ± 249	2.0 ± 4.5	3804 ± 911	▲388* ± 376	4156* ± 689	8.8	pg/mL
von Willebrand Factor (vWF)	4.03 ± 0.83	1.43§ ± 1.66	▲29.00 ± 3.16	▲21.00 ± 3.46	1.46 ± 2.04	1.58 ± 1.45	▲8.03* ± 1.51	▲7.46* ± 2.06	2.3	ng/mL

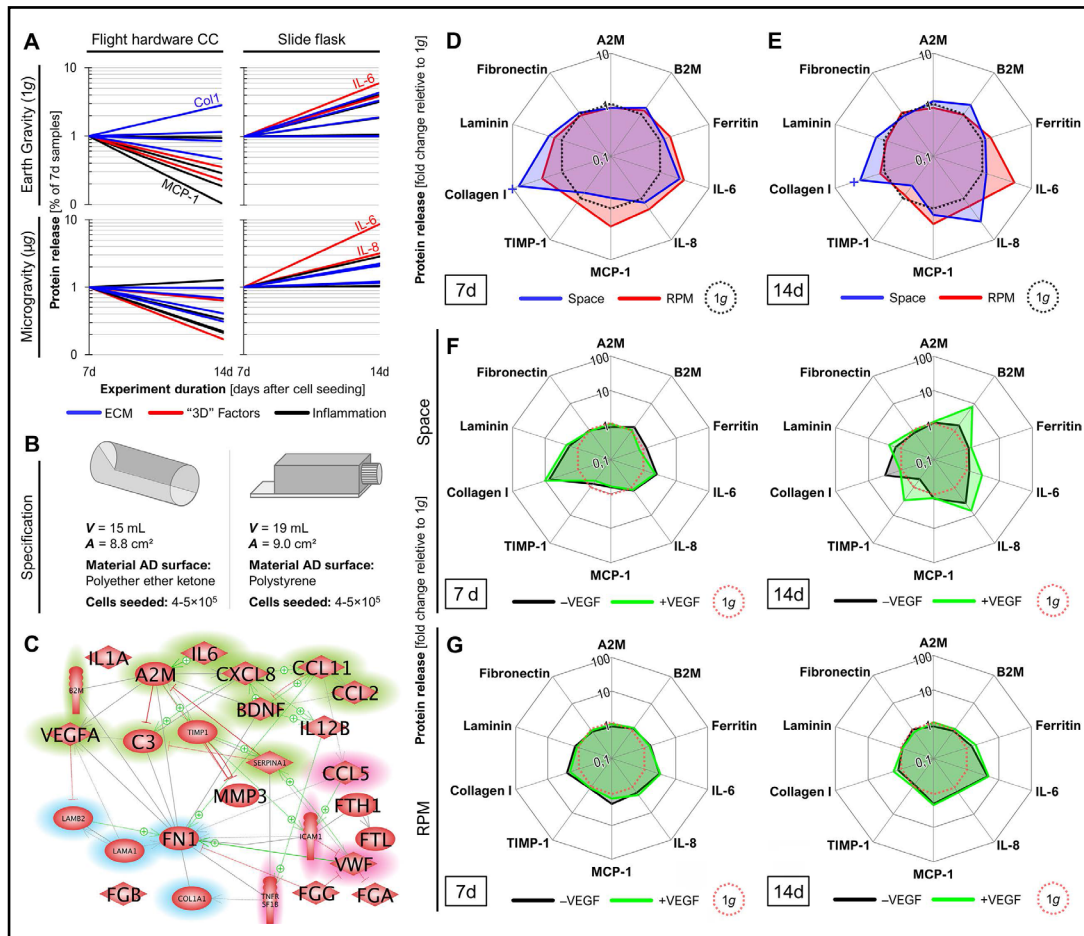


Fig. 4. Effects of microgravity on EC secretion behavior. A) Time courses of protein releases in the different cultivation chambers between day 7 and day 14. B) Specification of the constructed cultivation chamber and commercial slide flasks. C) Mutual interaction of proteins analyzed by MAP technology (InflammationMAP®). Green background indicates released factors both in the hardware and in slide flasks, red background shows factors only released in slide flasks. ECM components are highlighted in blue. The green arrows indicate activating and the red one inhibiting effects. The interaction network was built up using Elsevier Pathway Studio v.11. D, E) Protein release profiles of ECs cultured for 5 d and 12 d under r- and s-µg conditions. Fold changes of protein secretion compared to 1g controls are shown in blue (space samples) or in red (RPM samples). + marks the minimum fold change, as protein levels were below the LLOQ. The LLOQ was used for comparison. The black dotted lines indicate the secretion levels under 1g (control) conditions. F, G) Protein release profiles of ECs cultured for 5 d and 12 d in space (F) and on the RPM (G). Fold changes of protein secretion in presence of supplemented VEGF are shown in green, without additional VEGF in black. The red dotted lines indicate the secretion levels under 1g (control) conditions. * P < 0.05 vs. 1g.

factors and cytokines were investigated (Fig. 4A). α1-Antitrypsin (AAT), α2-Macroglobulin (A2M), β2-Microglobulin (B2M), Brain-Derived Neurotrophic Factor (BDNF), Complement C3, Eotaxin-1, Ferritin (FRTN), interleukins (IL)-1α, -6, -8, Monocyte Chemotactic Protein 1 (MCP-1), Tissue Inhibitor of Metalloproteinases 1 (TIMP-1), and VEGF could be determined in both types of cell containers. But detectable amounts of Intercellular Adhesion Molecule 1 (ICAM-1), Matrix Metalloproteinase-3 (MMP-3), T-Cell-Specific Protein RANTES, Tumor Necrosis Factor Receptor 2 (TNFR2), and von Willebrand Factor (vWF) were only found in slide flasks, while fibrinogen and IL-12 were detected in CC only. Regarding the amount of secreted proteins found in both types of chambers, it is obvious that higher amounts of B2M, IL-6, MCP-1 and TIMP-1 were secreted in slide flasks. But IL-8 (also called CXCL8, CXC-

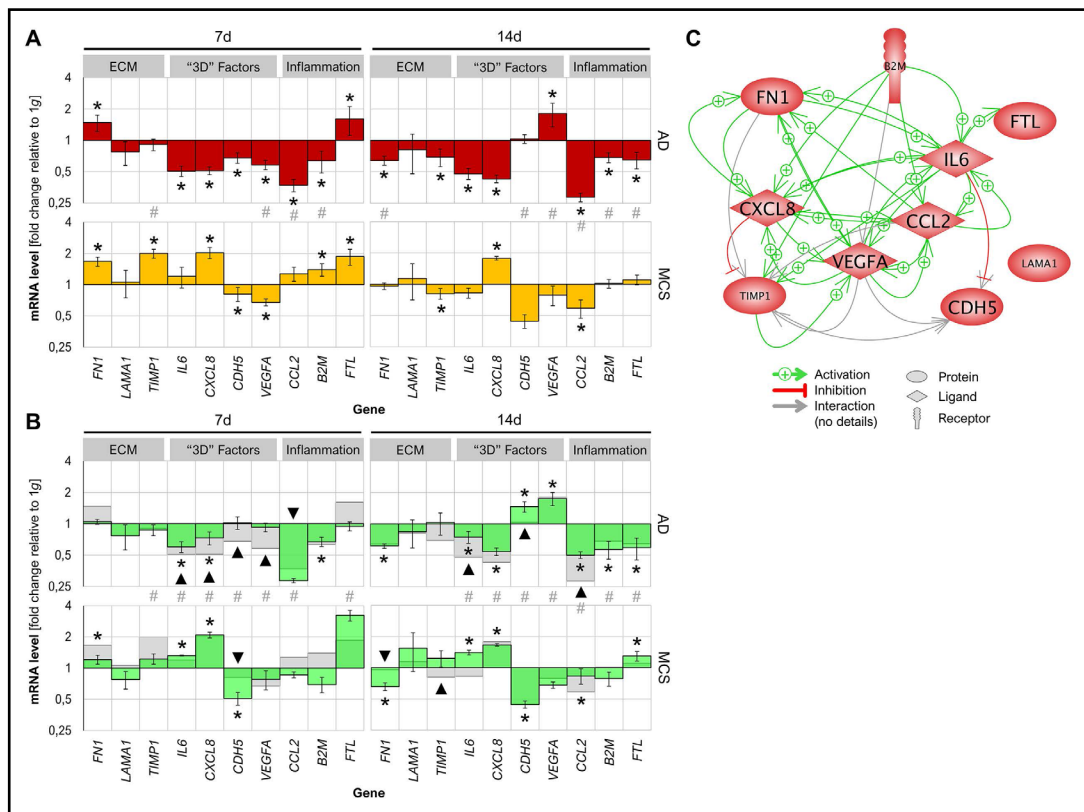


Fig. 5. Effects of $s\text{-}\mu\text{g}$ on the gene expression of EA.hy926 cells. A) Changes of mRNA levels after exposure to the RPM. Fold changes of AD cells are shown in red, fold changes of MCS are shown in yellow B) Changes of mRNA levels after VEGF supplementation (green bars) compared to samples without additional VEGF (grey bars). C) Mutual interaction of selected genes at gene expression level. We selected 10 genes, whose up- or down-regulation were analysed by qPCR after 14 d culturing on the RPM. The green arrows indicate activating and the red one inhibiting effects. The interaction network was built up using Elsevier Pathway Studio v.11. * $P < 0.05$ vs. $1g$ control; # $P < 0.05$ AD vs. MCS; ▼|▲ $P < 0.05$ vs. $-VEGF$.

Motiv-Chemokine 8) appeared to be higher concentrated in CC (Table 4 and 5). Taking the various values together, it was obvious that the different materials of CC (Fig. 4B, left side) and of slide flasks (Fig. 4B, right side) influenced the release of biological factors differently, although both kinds of material did not have any influence on viability or apoptosis of the cells [25]. Their interaction was given in Fig. 4C.

Fold changes of secreted proteins

For better visualization of further results shown within the tables, spider charts were generated, which give an overview on the culture condition dependent variation of the influence of μg and VEGF (Fig. 4D-G).

Selected components are compared regarding their release during one (Fig. 4D) or two weeks of spaceflight and RPM-culture (Fig. 4E). During the first week differences arose for MCP-1 and collagen I, while after a second week IL-6, IL-8 and collagen I differed in the amount of appearance within the culture supernatant, when their concentrations in the supernatant of spaceflight or RPM cultures were compared with those in the corresponding $1g$ controls. VEGF supplementation had little influence on the cells during the first week in space. During the second week in space, however, it boosted the release of B2M, IL-6, IL-8, and TIMP-1 but reduced collagen I secretion (Fig. 4F). When the cell cultures were incubated on the RPM, a significant influence of the presence of VEGF could not be detected (Fig. 4G).

Interaction of proteins released into the supernatant

In order to see whether there is a linkage between the proteins secreted into the culture supernatant, we performed an interaction analysis. Fig. 4C shows that most of the factors detected in the culture supernatants form a network of interaction. In this network ECM components (blue rim) determined by ELISA are embedded together with biological factors detected by the Human InflammationMAP®. Furthermore, the compounds secreted in the supernatant during culturing in both kinds of culture dish showed far branched relationships as indicated by the icons with a green rim for SERPINA1, A2M, B2M, BDNF, C3, CCL11 (eotaxin-1), IL-6, IL-8, CCL2 (MCP-1), TIMP-1, and VEGF-A. ICAM-1, MMP-3, TNFR2, CCL5 (RANTES) and vWF were detected only in supernatants of slide flasks. Of these factors ICAM-1, TNFR2, CCL5 (RANTES) and vWF are netted as indicated by icons with red rims. It is of interest that fibronectin (FN1), which is rather resistant to the influence of μg and VEGF-A, binds to Col1A1, that is up-regulated especially in space. But further explanations about the cells' μg dependent secretion behavior cannot be derived from their interaction network. Therefore, we also investigated the underlying network of genes.

Changes in gene expression

Unfortunately, the cell concentration found in the flight hardware after return was too low for transcriptional analysis by qPCR. Therefore, we investigated only the cells cultured on the RPM. Fig. 5A and 5B show that a number of genes (*TIMP1*, *IL6*, *CXCL8*, *CCL2*, *B2M*) are differently regulated in AD and MCS cells. While most of the investigated genes are down-regulated in AD cells, there is a considerable number of them up- or un-regulated in MCS cells (Table 6). This effect may be due to the kind of mutually up-building gene interaction shown in Fig. 5C. There is also an effect of duration of exposure to the RPM (*FN1*, *TIMP1*, *VEGFA*) and of the presence of supplemented VEGF. Only *LAMA1* was not significantly regulated under all culture conditions, but VEGF supplementation exerted its influence on the regulation of *FN1* already after 7 d (Table 6). There is little effect of the external VEGF on the *VEGFA* gene. Also IL-6 and IL-8 are regulated very similarly irrespective of the duration of RPM exposure or the presence of external VEGF. Most interesting are the effect of time of incubation and of VEGF on the regulation of *CDH5*, which may be important for spheroid formation. While after 7 d a divergence of regulation is visible in the presence of VEGF only, the divergence is enforced after 14 d. It is also interesting that *IL6*, which has an inhibitory influence on *CDH5* is up-regulated when *CDH5* is down-regulated (Fig. 5C, Table 6).

Discussion

In this study we investigated the influence of r- μg on EA.hy926 cells. For this purpose, we cultured cells for 5 d and 12 d (previous studies in s- μg suggested that these two time points are most interesting to observe μg -dependent changes in phenotype/growth behavior [7, 19]) under r- μg in space either in plain culture medium or in medium containing VEGF. Subsequently, we determined the growth pattern and quantities of growth factors/cytokines secreted and performed comparative experiments using the same timeline and temperature protocols as in the space experiment, but keeping the cells either on an RPM or under normal 1g laboratory conditions.

Three-dimensional growth in real (r- μg) and simulated microgravity (s- μg)

In space we observed similar 3D growth as observed in several studies using s- μg before. Examining the cells subjected to r- μg in space we detected three different populations of EA.hy926 cells. Some ECs remained adherent (Fig. 3C), but others had assembled to 3D structures either with spherical or with tube-like appearance (Fig. 3D-F). This demonstrates that EA.hy926 cells exhibit 3D growth in space, where r- μg is a long-term condition that cannot be found on Earth. Hence, they behave similarly like human FTC-133 thyroid cells [39], bovine articular chondrocytes [40], or pig liver stem cells [41] which already showed

Table 6. Gene expression of EA.hy926 cells after exposure to the RPM compared with 1g controls. Cells were cultured in slide flasks. The data was generated by using qPCR. Values are given as mean ± SD; *: P <0.05 vs. 1g; ▼|▲: P <0.05 vs. 7d; §: P <0.05 vs. -VEGF; #: P <0.05 vs. AD; AD: Adherently growing cells; MCS: Multicellular spheroids; n.d.: not detectable. *18S* was used as housekeeper. *LAMB2* (Laminin Subunit β2), *COL1A1* (Collagen Type I α1 Chain), and *CCL11* (Eotaxin-1) mRNA levels were below the LLOQ

Function	Gene Symbol	Encoded Protein	Earth gravity (1g)				RPM (s-μg)				Morphology
			7 d		14 d		7 d		14 d		
			- VEGF	+ VEGF	- VEGF	+ VEGF	- VEGF	+ VEGF	- VEGF	+ VEGF	
Extracellular Matrix (ECM)	<i>FN1</i>	Fibronectin					167.2' ± 16.85	150.2* ± 14.78	▼137.5* ± 10.08	▼110.5* ± 9.61	MCS
			100.0 ± 10.70	124.5§ ± 8.49	▲143.6 ± 8.42	▲168.0 ± 24.06	148.0' ± 26.25	130.2 ± 6.85	▼91.96' ± 8.95	▼102.8' ± 5.11	AD
	<i>LAMA1</i>	Laminin Subunit α1					105.9 ± 31.45	87.66 ± 16.73	▼31.47 ± 11.96	▼36.46* ± 14.77	MCS
			100.0 ± 26.46	112.9 ± 20.34	▼27.59 ± 5.38	▼23.61 ± 5.83	77.38 ± 19.86	86.65 ± 23.45	▼22.48 ± 9.26	▼19.80 ± 5.95	AD
	<i>TIMP1</i>	Tissue Inhibitor of Metalloproteinases 1					199.9* ± 19.81	199.6* ± 22.85	▼67.54' ± 8.10	▼93.75§ ± 16.97	MCS
			100.0 ± 19.25	162.5§ ± 10.50	83.12 ± 10.06	▼75.83 ± 12.06	91.12 ± 11.48	141.8§ ± 16.83	▼57.54' ± 11.04	▼77.85§ ± 18.78	AD
<i>IL6</i>	Interleukin-6					119.8* ± 26.70	201.7* ± 1.81	▲174.0* ± 19.56	▲273.7* ± 15.22	MCS	
		100.0 ± 22.57	152.8§ ± 16.63	▲210.5 ± 43.73	▲195.5 ± 28.29	50.68' ± 5.84	91.55§ ± 11.00	▲100.7' ± 12.22	▲146.0§ ± 19.13	AD	
"3D" Factors	<i>CXCL8</i>	Interleukin-8					202.5* ± 26.37	314.5* ± 20.41	▲710.0* ± 31.05	▲654.7* ± 19.78	MCS
			100.0 ± 12.26	151.1§ ± 6.50	▲398.4 ± 54.49	▲393.1 ± 7.82	51.10' ± 4.35	110.2§ ± 15.75	▲170.3' ± 14.19	▲212.7' ± 17.90	AD
	<i>CDH5</i>	VE-Cadherin					81.23' ± 12.45	62.56* ± 8.66	65.20* ± 9.79	52.53* ± 4.14	MCS
			100.0 ± 11.17	123.0 ± 19.18	▲147.6 ± 26.05	119.0 ± 25.54	67.89' ± 7.72	126.0§ ± 17.28	▲152.8 ± 15.27	▲173.8 ± 20.09	AD
	<i>VEGFA</i>	Vascular Endothelial Growth Factor A					67.39* ± 5.17	77.92* ± 16.18	▲121.4* ± 25.96	▲104.8* ± 7.64	MCS
			100.0 ± 14.70	131.9 ± 22.85	▲153.8 ± 44.46	▲188.6 ± 23.48	58.15' ± 5.79	92.41§ ± 8.66	▲278.1' ± 71.17	▲268.0' ± 39.0	AD
Inflammation	<i>B2M</i>	β2-Microglobulin					139.4* ± 9.72	97.20 ± 16.32	▲356.2* ± 34.81	▲301.6* ± 46.12	MCS
			100.0 ± 17.67	140.0§ ± 18.85	▲351.1 ± 28.46	▲383.7 ± 84.58	63.54' ± 15.02	94.19§ ± 9.86	▲240.6' ± 26.01	▲217.6' ± 41.83	AD
	<i>CCL2</i>	Monocyte Chemoattractant Protein 1 (MCP-1)					127.2* ± 19.20	144.9* ± 9.64	▼40.05* ± 8.00	▼47.76* ± 8.08	MCS
			100.0 ± 14.38	167.9§ ± 13.54	▼68.08 ± 17.08	▼57.48 ± 8.18	37.05' ± 4.94	47.79§ ± 2.28	▼19.33' ± 1.86	▼28.80§ ± 2.06	AD
	<i>FTL</i>	Ferritin Light Chain					186.3' ± 32.54	402.4* ± 47.19	▲320.2* ± 35.14	344.9* ± 36.86	MCS
			100.0 ± 20.05	124.9 ± 11.66	▲290.1 ± 62.73	▲266.1 ± 42.59	161.2' ± 49.54	118.1 ± 11.42	188.2 ± 33.70	157.2' ± 36.99	AD

organoid formation during space missions. On Earth long-term $s\text{-}\mu\text{g}$ can be simulated with the help of instruments like the 2D-clinostat, the Rotating Wall Vessel, and the RPM or by using magnetic levitation [42-44]. We used the RPM as it provides high quality $s\text{-}\mu\text{g}$ inside the whole cell culture flask, for both adherent and floating cells as well as for spheroids. Even the simulation triggers ECs to exhibit 3D growth (Fig. 3G), when cells are exposed to a random change in direction of the gravitational pull preventing sedimentation which over time corresponds to a 'quasi-microgravity' [28], reaching a calculated quality of 10^{-3} to $10^{-4} g$ with our RPM [29]. This reduction of gravity forces not only changed the growth behavior of ECs, but triggers also 3D growth of thyroid (cancer) cells [36], breast cancer cells [45] or chondrocytes [46].

In addition to μg , a space experiment is accompanied by multiple other factors, such as cosmic radiation, mechanical stress at the rocket launch, temperature fluctuations during the transport to the ISS and special CCs consisting of PEEK instead of polystyrene [25, 39]. Even vibration and hyper- g during the rocket launch can affect ECs on the transcriptional and translational level [11, 47, 48]. These factors, however, do not prevent 3D growth. Hence, prevention of sedimentation is the major cause that allows at least a group of cells to leave the monolayer and to assemble to 3D structures. This holds true in space as well as on suitable ground-based devices like the RPM. As the latter technology is cheaper and more often applicable than spaceflights, still inducing 3D growth similar to a stay in space, it can now be used with more confidence to learn about the mechanism of scaffold-free tissue formation under μg .

Protein secretion and the influence of the hardware

Little is known about the proteins involved in μg -dependent formation of tube-like structures by ECs [7, 8]. In human cancer cells we have already recognized several growth factors and proteins of the focal adhesion complex and of tight junctions playing a role in MCS formation [49, 50]. In these experiments we focused on components of the ECM (Tables 2, 3) as well as growth factors and cytokines released into the supernatant (Tables 4, 5). We studied their release by cells enclosed in flight hardware CCs or in polystyrene slide flasks as used for RPM experiments. Both types of cell containers were either kept under μg (flight hardware in $r\text{-}\mu\text{g}$, polystyrene flask in $s\text{-}\mu\text{g}$ on the RPM) as well as under $1g$ control conditions, respectively. Although 3D structures were found in both containers (Fig. 3), when cultured under μg , we recognized container dependent differences in the release of proteins.

Significantly higher quantities of the ECM components fibronectin, laminin, and collagen I were detected in the supernatants of slide flasks than in those of space hardware CCs, independently whether the samples had been incubated under gravity or under μg . (Tables 2, 3). Interestingly, a clear influence of gravity on the amounts of soluble ECM is only detected for collagen I. Type I collagen is the most abundant collagen of the human body [51]. Collagen metabolism in the ECM is related to the pathogenesis of cardiovascular stiffness [52, 53]. Astronauts returning from space do suffer from an increased arterial stiffness [54]. In addition, an increased procollagen level was found in the skin of mice living for 3 months on the ISS [55]. Hence, our *in vitro* result could represent a space-dependent effect. The ECM plays a crucial role in 3D growth and angiogenesis [56-58]. Infanger *et al.* have reported previously that $s\text{-}\mu\text{g}$ can enhance the expression of collagen I, laminin, and fibronectin in EA.hy926 cells [8]. In their experiments VEGF supplementation showed some effect during the first 4 h, but then the VEGF influence ceased and seemed to suppress the μg -dependent amounts of ECM proteins [8].

As ECM components secreted by tissue cells are at least in part adsorbed by the CC material to form an anchorage possibility for the cells or incorporated in 3D structures, it is difficult to decide whether the different quantities of the components dissolved in the supernatant are due to a different production activity of the cells or to different adsorption by the chamber material. For example, intracellular levels of ECM proteins determined after long-term experiments on the RPM indicated significant increases of laminin and fibronectin

in tube-like structures after 28 d [7] and a significant increase of fibronectin was found in MCS after 35 d [21]. In any case, our experiments suggest a relationship between the dissolved ECM components and cytokines. A clear cell container material-dependent difference was found in quantities of a number of cytokines/growth factors released into supernatant by ECs (Fig. 4A, B). This is corroborated by a recent study by Cazzaniga and coworkers, who reported that hardware designed for spaceflights can impact cell behavior [59]. But it is not clear which cytokine is directly affected by the chamber material and which is regulated by the network of interaction shown in Fig. 4C. Only the A2M quantities detected were similar under all incubation conditions.

Impact of VEGF supplementation

We observed a low VEGF production in space hardware and polystyrene flasks under 1g. This may be explained as VEGF is an important growth and survival factor for ECs [60], which is secreted by a variety of cell types, but not by ECs themselves [61]. Significantly enhanced amounts of VEGF were only found in supernatants of RPM cultures. This observation could be due to the nature of EA.hy926 cells, which are hybrid cells consisting of endothelial and of cancer cells [62] as well as due to mechanical stimuli, whose effects on VEGF have been demonstrated for different cell types [63-65].

In vivo, VEGF takes part in promoting angiogenesis by stimulation of survival, permeability, migration, and proliferation [66]. In flight hardware samples, VEGF supplementation made C3, eotaxin-1, fibrinogen, and IL-1a detectable and decreased B2M, IL-8 and TIMP-1 levels under 1g, while IL-6 was increased under μg (Table 4, Fig. 4F). In polystyrene chambers, VEGF supplementation made eotaxin-1 visible after 7 d and 14 d but ICAM-1 after 14 d under 1g and under μg (Table 5, Fig. 4G). A relationship between enhancement of VEGF, collagen I and eotaxin-1 has been described for airway smooth muscle cells [67]. Although a role of eotaxin-1 in *in vitro* scaffold-free tube formation has not been described yet, it appears to support cancer dependent angiogenesis [68].

IL-6 and IL-8

Interleukins 6 and 8 are well known candidates in analyses of μg studies. Enhancement of IL-6 and IL-8 production under μg conditions has been reported before for EA.hy926 cells [21, 23], and different malignant and non-malignant human cell lines [45, 69, 70]. IL-8 was identified to be a potent autocrine growth and survival factor for ECs [71]. It regulates angiogenesis and modulates endothelial cell-cell-connections by temporarily down-regulation of tight junctions but not by integrin-mediated focal adhesions [72]. In our experiments, after a 7 day culture the IL-8 concentration was found higher in the supernatants of flight hardware cultures than in those of polystyrene cultures (Tables 4, 5). During the second week the IL-8 concentration declined in the first type of cell containers, while it increased in polystyrene cultures. At that time the μg effect was most prominent in the flight hardware chamber (Fig. 4D, E), resembling that of B2M, a protein which is expressed at a constant level in many cells [73]. B2M was described as a common γ radiation responder [74]. Its response to space conditions may therefore be contributed to an irradiation effect, while the role of IL-8 needs further investigation. In these experiments, the IL-6 secretion was clearly enhanced under r- μg in flight hardware CCs as well as in polystyrene culture flasks, when 3D structures were formed. However, the μg effect was time shifted. It was most prominent after 7 d on the flight hardware and after 14 d on the RPM (Fig. 4D, E). Time shifts in tube formation were already observed when microvascular ECs and EA.hy926 cells were investigated comparatively [24]. IL-6 has also been reported to induce ferritin synthesis [75]. This fits very well with the results of tables 4 and 5.

Source of cytokines/growth factors

Two other interesting proteins observed were MCP-1 and TIMP-1. Their secretion depended on the cell container material, similar to the one of IL-8 and B2M. However, these proteins did not show any response to μg . Therefore, combining the cell culture supernatants

analysis, one may conclude that considering the influence of the material of the culture dishes, the IL-6 concentration in the culture supernatants are most closely related to 3D structure formation. However, proteins detected in a culture supernatant may be released by both, the adherent and the 3D structure cells (Fig. 3C-F). In order to get an impression which cell type is responsible for a current concentration of a cytokine, growth factor or ECM component, we performed qPCR analyses on ten selected genes of which 9 form an interaction network (Fig. 5). As mentioned above, the analyses were performed only on RPM samples, due to a lack of the space sample material. At a first glance it can be seen that only *FN1*, *CDH5*, *VEGFA* and *FTL* genes share a similar activation status in adherent and 3D structure cells after 7 d, while *TIMP1*, *IL6* and *CCL2* showed these features after two weeks. Addition of VEGF to the culture medium changed the gene expression for *LAMA1*, *CDH5*, *CCL2*, *B2M* and *FTL* after 7 d and for *FN1*, *TIMP1*, *IL6*, *CDH5* and *B2M* after two weeks. The qPCR analyses clearly show that further work is required to identify the source of the various cytokines, growth factors and ECM components.

Conclusion

Using an automatic flight hardware, specially designed for space experiments, we demonstrated for the first time that ECs exhibit 3D growth in space. This indicates that μg may be the major cause for the formation of tube-like aggregates of ECs and justifies the use of RPM for studies on scaffold free 3D structure formation, when the importance of the material of cell containers is considered. In this study it was clearly demonstrated that the material of the cell containers influences the protein secretion of ECs. A further influence on 3D formation cannot be excluded, as very large spheroids were detected when thyroid cancer cells had been sent to space [76]. IL-6 is more and more emerging as a key protein in μg dependent 3D formation. It is up-regulated, when 3D structures are formed and down-regulate VE-cadherin weakening tight junctions, like E-cadherin in breast cancer cells [49]. Taken together, the SPHEROIDS experiments increased our knowledge of EC behavior in space. Aiming to better understand *in vitro* angiogenesis and to improve tissue engineering with ECs, it will be of interest to study the interplay of cells leaving the monolayer for 3D structure formation with those remaining in the monolayer.

Abbreviations

μg (Microgravity); 1g (Earth gravity); 3D (Three-dimensional); CC (Cell cultivation chamber (flight hardware)); EC (Endothelial cell); ECM (Extracellular matrix); IL (Interleukin); ISS (International Space Station); MAP (Multi-Analyte Profiling); MCS (Multicellular spheroid); PEEK (Polyether ether ketone); RPM (Random Positioning Machine); VEGF (Vascular endothelial growth factor A).

Acknowledgements

The authors would like to thank Jason Hatton, Nadine Boersma and Andrea Koehler from ESA, Raimondo Fortezza from Telespazio, Stefan Riwaltdt, Christin Baake, Daniel Echegoyen, and Lasse Slumstrup for their support of the space experiment. We like to thank Christa Baumann (University of Regensburg) for performing the paraffin embedding and histochemical stains of the space spheroids. The research was supported by the German Space Agency (DLR, grants 50BW1124 and 50BW1524), the European Space Agency (ESA, grant ESA-AO-2004-PCP-006) as well as BELSPO PRODEX (IMPULSE 2 grant 4000109861).

Disclosure Statement

Competing financial interests: The authors declare no competing financial interests. The views expressed herein can in no way be taken to reflect the official opinion of the European Space Agency.

References

- 1 White RJ, Averner M: Humans in space. *Nature* 2001;409:1115.
- 2 Buckley JC, Jr., Lane LD, Levine BD, Watenpaugh DE, Wright SJ, Moore WE, Gaffney FA, Blomqvist CG: Orthostatic intolerance after spaceflight. *J Appl Physiol* 1996;81:7-18.
- 3 Delp MD, Charvat JM, Limoli CL, Globus RK, Ghosh P: Apollo Lunar Astronauts Show Higher Cardiovascular Disease Mortality: Possible Deep Space Radiation Effects on the Vascular Endothelium. *Sci Rep* 2016;6:29901.
- 4 Nicogossian AE, Charles JB, Bungo MW, Leach-Huntoon CS, Nicogossian AE: Cardiovascular function in space flight. *Acta Astronaut* 1991;24:323-328.
- 5 Sato M, Ohashi T: Biorheological views of endothelial cell responses to mechanical stimuli. *Biorheology* 2005;42:421-441.
- 6 Maier JA, Cialdai F, Monici M, Morbidelli L: The impact of microgravity and hypergravity on endothelial cells. *Biomed Res Int* 2015;2015:434803.
- 7 Grimm D, Infanger M, Westphal K, Ulbrich C, Pietsch J, Kossmehl P, Vadrucci S, Baatout S, Flick B, Paul M, Bauer J: A delayed type of three-dimensional growth of human endothelial cells under simulated weightlessness. *Tissue Eng Part A* 2009;15:2267-2275.
- 8 Infanger M, Kossmehl P, Shakibaei M, Baatout S, Witzing A, Grosse J, Bauer J, Cogoli A, Faramarzi S, Derradji H, Neefs M, Paul M, Grimm D: Induction of three-dimensional assembly and increase in apoptosis of human endothelial cells by simulated microgravity: impact of vascular endothelial growth factor. *Apoptosis* 2006;11:749-764.
- 9 Janmaleki M, Pachenari M, Seyedpour SM, Shahghadami R, Sanati-Nezhad A: Impact of Simulated Microgravity on Cytoskeleton and Viscoelastic Properties of Endothelial Cell. *Sci Rep* 2016;6:32418.
- 10 Versari S, Longinotti G, Barenghi L, Maier JA, Bradamante S: The challenging environment on board the International Space Station affects endothelial cell function by triggering oxidative stress through thioredoxin interacting protein overexpression: the ESA-SPHINX experiment. *FASEB J* 2013;27:4466-4475.
- 11 Wehland M, Ma X, Braun M, Hauslage J, Hemmersbach R, Bauer J, Grosse J, Infanger M, Grimm D: The impact of altered gravity and vibration on endothelial cells during a parabolic flight. *Cell Physiol Biochem* 2013;31:432-451.
- 12 Li N, Wang C, Sun S, Zhang C, Lü D, Chen Q, Long M: Microgravity-Induced Alterations of Inflammation-Related Mechanotransduction in Endothelial Cells on Board SJ-10 Satellite. *Front Physiol* 2018;9:1025.
- 13 Ingber DE: Tensegrity: the architectural basis of cellular mechanotransduction. *Annu Rev Physiol* 1997;59:575-599.
- 14 Griffoni C, Di Molfetta S, Fantozzi L, Zanetti C, Pippia P, Tomasi V, Spisni E: Modification of proteins secreted by endothelial cells during modeled low gravity exposure. *J Cell Biochem* 2011;112:265-272.
- 15 Versari S, Villa A, Bradamante S, Maier JAM: Alterations of the actin cytoskeleton and increased nitric oxide synthesis are common features in human primary endothelial cell response to changes in gravity. *Biochim Biophys Acta* 2007;1773:1645-1652.
- 16 Morbidelli L, Monici M, Marziliano N, Cogoli A, Fusi F, Waltenberger J, Ziche M: Simulated hypogravity impairs the angiogenic response of endothelium by up-regulating apoptotic signals. *Biochem Biophys Res Commun* 2005;334:491-499.
- 17 Carlsson SIM, Bertilaccio MTS, Ballabio E, Maier JAM: Endothelial stress by gravitational unloading: effects on cell growth and cytoskeletal organization. *Biochim Biophys Acta* 2003;1642:173-179.
- 18 Infanger M, Ulbrich C, Baatout S, Wehland M, Kreutz R, Bauer J, Grosse J, Vadrucci S, Cogoli A, Derradji H, Neefs M, Kusters S, Spain M, Paul M, Grimm D: Modeled gravitational unloading induced downregulation of endothelin-1 in human endothelial cells. *J Cell Biochem* 2007;101:1439-1455.

- 19 Grimm D, Bauer J, Ulbrich C, Westphal K, Wehland M, Infanger M, Aleshcheva G, Pietsch J, Ghardi M, Beck M, El-Saghire H, de Saint-Georges L, Baatout S: Different responsiveness of endothelial cells to vascular endothelial growth factor and basic fibroblast growth factor added to culture media under gravity and simulated microgravity. *Tissue Eng Part A* 2010;16:1559-1573.
- 20 Ulbrich C, Westphal K, Baatout S, Wehland M, Bauer J, Flick B, Infanger M, Kreutz R, Vadrucci S, Egli M, Cogoli A, Derradji H, Pietsch J, Paul M, Grimm D: Effects of basic fibroblast growth factor on endothelial cells under conditions of simulated microgravity. *J Cell Biochem* 2008;104:1324-1341.
- 21 Dittrich A, Grimm D, Sahana J, Bauer J, Krüger M, Infanger M, Magnusson NE: Key Proteins Involved in Spheroid Formation and Angiogenesis in Endothelial Cells After Long-Term Exposure to Simulated Microgravity. *Cell Physiol Biochem* 2018;45:429-445.
- 22 Gapizov SS, Petrovskaya LE, Shingarova LN, Svirschevskaya EV, Dolgikh DA, Kirpichnikov MP: The Effect of TNF and VEGF on the Properties of Ea.hy926 Endothelial Cells in a Model of Multi-Cellular Spheroids. *Acta Naturae* 2018;10:34-42.
- 23 Ma X, Wehland M, Schulz H, Saar K, Hübner N, Infanger M, Bauer J, Grimm D: Genomic Approach to Identify Factors That Drive the Formation of Three-Dimensional Structures by EA.hy926 Endothelial Cells. *PLoS ONE* 2013;8:e64402.
- 24 Ma X, Sickmann A, Pietsch J, Wildgruber R, Weber G, Infanger M, Bauer J, Grimm D: Proteomic differences between microvascular endothelial cells and the EA.hy926 cell line forming three-dimensional structures. *Proteomics* 2014;14:689-698.
- 25 Pietsch J, Gass S, Nebuloni S, Echegoyen D, Riwaldt S, Baake C, Bauer J, Corydon TJ, Egli M, Infanger M, Grimm D: Three-dimensional growth of human endothelial cells in an automated cell culture experiment container during the SpaceX CRS-8 ISS space mission - The SPHEROIDS project. *Biomaterials* 2017;124:126-156.
- 26 Edgell CJ, McDonald CC, Graham JB: Permanent cell line expressing human factor VIII-related antigen established by hybridization. *Proc Natl Acad Sci U S A* 1983;80:3734-3737.
- 27 Ahn K, Pan S, Beningo K, Hupe D: A permanent human cell line (EA.hy926) preserves the characteristics of endothelin converting enzyme from primary human umbilical vein endothelial cells. *Life Sci* 1995;56:2331-2341.
- 28 van Loon JJWA: Some history and use of the random positioning machine, RPM, in gravity related research. *Adv Space Res* 2007;39:1161-1165.
- 29 Borst AG, van Loon JJWA: Technology and Developments for the Random Positioning Machine, RPM. *Microgravity Sci Technol* 2008;21:287.
- 30 Ma X, Wehland M, Schulz H, Saar K, Hübner N, Infanger M, Bauer J, Grimm D: Genomic approach to identify factors that drive the formation of three-dimensional structures by EA.hy926 endothelial cells. *PLoS One* 2013;8:e64402.
- 31 Ulbrich C, Westphal K, Pietsch J, Winkler HD, Leder A, Bauer J, Kossmehl P, Grosse J, Schoenberger J, Infanger M, Egli M, Grimm D: Characterization of human chondrocytes exposed to simulated microgravity. *Cell Physiol Biochem* 2010;25:551-560.
- 32 Wüest SL, Richard S, Kopp S, Grimm D, Egli M: Simulated microgravity: critical review on the use of random positioning machines for mammalian cell culture. *Biomed Res Int* 2015;2015:971474.
- 33 Riwaldt S, Monici M, Graver Petersen A, Birk Jensen U, Evert K, Pantalone D, Utpatel K, Evert M, Wehland M, Krüger M, Kopp S, Frandsen S, Corydon T, Sahana J, Bauer J, Lützenberg R, Infanger M, Grimm D: Preparation of A Spaceflight: Apoptosis Search in Sutured Wound Healing Models. *Int J Mol Sci* 2017;18(12):2604.
- 34 Grimm D, Jabusch HC, Kossmehl P, Huber M, Fredersdorf S, Griese DP, Kramer BK, Kromer EP: Experimental diabetes and left ventricular hypertrophy: effects of beta-receptor blockade. *Cardiovasc Pathol* 2002;11:229-237.
- 35 Grosse J, Warnke E, Pohl F, Magnusson NE, Wehland M, Infanger M, Eilles C, Grimm D: Impact of sunitinib on human thyroid cancer cells. *Cell Physiol Biochem* 2013;32:154-170.
- 36 Kopp S, Warnke E, Wehland M, Aleshcheva G, Magnusson NE, Hemmersbach R, Corydon TJ, Bauer J, Infanger M, Grimm D: Mechanisms of three-dimensional growth of thyroid cells during long-term simulated microgravity. *Sci Rep* 2015;5:16691.

- 37 Rothermund L, Kreutz R, Kossmehl P, Fredersdorf S, Shakibaei M, Schulze-Tanzil G, Paul M, Grimm D: Early onset of chondroitin sulfate and osteopontin expression in angiotensin II-dependent left ventricular hypertrophy. *Am J Hypertens* 2002;15:644-652.
- 38 ESA. Kubik Description. Available online: http://esamultimedia.esa.int/docs/hsf_research/Kubik_description.pdf.
- 39 Pietsch J, Ma X, Wehland M, Aleshcheva G, Schwarzwälder A, Segerer J, Birmem M, Horn A, Bauer J, Infanger M, Grimm D: Spheroid formation of human thyroid cancer cells in an automated culturing system during the Shenzhou-8 Space mission. *Biomaterials* 2013;34:7694-7705.
- 40 Freed LE, Langer R, Martin I, Pellis NR, Vunjak-Novakovic G: Tissue engineering of cartilage in space. *Proc Natl Acad Sci U S A* 1997;94:13885-13890.
- 41 Talbot NC, Caperna TJ, Blomberg L, Graninger PG, Stodieck LS: The effects of space flight and microgravity on the growth and differentiation of PICM-19 pig liver stem cells. *In vitro Cell Dev Biol Anim* 2010;46:502-515.
- 42 Herranz R, Anken R, Boonstra J, Braun M, Christianen PCM, de Geest M, Hauslage J, Hilbig R, Hill RJA, Lebert M, Medina FJ, Vagt N, Ullrich O, van Loon JJWA, Hemmersbach R: Ground-Based Facilities for Simulation of Microgravity: Organism-Specific Recommendations for Their Use, and Recommended Terminology. *Astrobiology* 2013;13:1-17.
- 43 Wüest SL, Richard S, Kopp S, Grimm D, Egli M: Simulated Microgravity: Critical Review on the Use of Random Positioning Machines for Mammalian Cell Culture. *Biomed Res Int* 2015;2015:971474.
- 44 Becker JL, Souza GR: Using space-based investigations to inform cancer research on Earth. *Nat Rev Canc* 2013;13:315-327.
- 45 Kopp S, Slumstrup L, Corydon TJ, Sahana J, Aleshcheva G, Islam T, Magnusson NE, Wehland M, Bauer J, Infanger M, Grimm D: Identifications of novel mechanisms in breast cancer cells involving duct-like multicellular spheroid formation after exposure to the Random Positioning Machine. *Sci Rep* 2016;6:26887.
- 46 Aleshcheva G, Bauer J, Hemmersbach R, Slumstrup L, Wehland M, Infanger M, Grimm D: Scaffold-free Tissue Formation Under Real and Simulated Microgravity Conditions. *Basic Clin Pharmacol Toxicol* 2016;119:26-33.
- 47 Costa-Almeida R, Carvalho DTO, Ferreira MJS, Aresta G, Gomes ME, van Loon JJWA, Van der Heiden K, Granja PL: Effects of hypergravity on the angiogenic potential of endothelial cells. *J R Soc Interface* 2016;13:pii:20160688.
- 48 Morbidelli L, Marziliano N, Basile V, Pezzatini S, Romano G, Conti A, Monici M: Effect of Hypergravity on Endothelial Cell Function and Gene Expression. *Microgravity Sci Technol* 2009;21:135-140.
- 49 Sahana J, Nassef MZ, Wehland M, Kopp S, Krüger M, Corydon TJ, Infanger M, Bauer J, Grimm D: Decreased E-Cadherin in MCF7 Human Breast Cancer Cells Forming Multicellular Spheroids Exposed to Simulated Microgravity. *Proteomics* 2018:e1800015.
- 50 Bauer J, Kopp S, Schlagberger EM, Grosse J, Sahana J, Riwaldt S, Wehland M, Luetzenberg R, Infanger M, Grimm D: Proteome Analysis of Human Follicular Thyroid Cancer Cells Exposed to the Random Positioning Machine. *Int J Mol Sci* 2017;18:pii:E546.
- 51 Shoulders MD, Raines RT: Collagen structure and stability. *Annu Rev Biochem* 2009;78:929-958.
- 52 Kohn JC, Lampi MC, Reinhart-King CA: Age-related vascular stiffening: causes and consequences. *Front Genet* 2015;6:112.
- 53 McNulty M, Mahmud A, Spiers P, Feely J: Collagen type-I degradation is related to arterial stiffness in hypertensive and normotensive subjects. *J Hum Hypertens* 2006;20:867-873.
- 54 Hughson RL, Robertson AD, Arbeille P, Shoemaker JK, Rush JW, Fraser KS, Greaves DK: Increased postflight carotid artery stiffness and in-flight insulin resistance resulting from 6-mo spaceflight in male and female astronauts. *Am J Physiol Heart Circ Physiol* 2016;310:H628-638.
- 55 Neutelings T, Nussgens BV, Liu Y, Tavella S, Ruggiu A, Cancedda R, Gabriel M, Colige A, Lambert C: Skin physiology in microgravity: a 3-month stay aboard ISS induces dermal atrophy and affects cutaneous muscle and hair follicles cycling in mice. *Npj Microgravity* 2015;1:15002.
- 56 Mongiat M, Andreuzzi E, Tarticchio G, Paulitti A: Extracellular Matrix, a Hard Player in Angiogenesis. *Int J Mol Sci* 2016;17:pii:1822.
- 57 Hynes RO: The extracellular matrix: not just pretty fibrils. *Science* 2009;326:1216-1219.

- 58 Sottile J: Regulation of angiogenesis by extracellular matrix. *Biochim Biophys Acta* 2004;1654:13-22.
- 59 Cazzaniga A, Moscheni C, Maier JAM, Castiglioni S: Culture of human cells in experimental units for spaceflight impacts on their behavior. *Exp Biol Med* 2017;242:1072-1078.
- 60 Ferrara N, Henzel WJ: Pituitary follicular cells secrete a novel heparin-binding growth factor specific for vascular endothelial cells. *Biochem Biophys Res Commun* 1989;161:851-858.
- 61 Berse B, Brown LF, Water LVD, Dvorak HF, Senger DR: Vascular permeability factor (vascular endothelial growth factor) gene is expressed differentially in normal tissues, macrophages, and tumors. *Mol Biol Cell* 1992;3:211-220.
- 62 Lieber M, Smith B, Szakal A, Nelson-Rees W, Todaro G: A continuous tumor-cell line from a human lung carcinoma with properties of type II alveolar epithelial cells. *Int J Cancer* 1976;17:62-70.
- 63 dela Paz NG, Walshe TE, Leach LL, Saint-Geniez M, D'Amore PA: Role of shear-stress-induced VEGF expression in endothelial cell survival. *J Cell Sci* 2012;125:831-843.
- 64 Milkiewicz M, Brown MD, Egginton S, Hudlicka O: Association between shear stress, angiogenesis, and VEGF in skeletal muscles *in vivo*. *Microcirculation* 2001;8:229-241.
- 65 Corydon TJ, Mann V, Slumstrup L, Kopp S, Sahana J, Askou AL, Magnusson NE, Echegoyen D, Bek T, Sundaresan A, Riwaldt S, Bauer J, Infanger M, Grimm D: Reduced Expression of Cytoskeletal and Extracellular Matrix Genes in Human Adult Retinal Pigment Epithelium Cells Exposed to Simulated Microgravity. *Cell Physiol Biochem* 2016;40:1-17.
- 66 Infanger M, Grosse J, Westphal K, Leder A, Ulbrich C, Paul M, Grimm D: Vascular endothelial growth factor induces extracellular matrix proteins and osteopontin in the umbilical artery. *Ann Vasc Surg* 2008;22:273-284.
- 67 Chan V, Burgess JK, Ratoff JC, O'Connor B J, Greenough A, Lee TH, Hirst SJ: Extracellular matrix regulates enhanced eotaxin expression in asthmatic airway smooth muscle cells. *Am J Respir Crit Care Med* 2006;174:379-385.
- 68 Wagsater D, Lofgren S, Hugander A, Dienus O, Dimberg J: Analysis of single nucleotide polymorphism in the promoter and protein expression of the chemokine eotaxin-1 in colorectal cancer patients. *World J Surg Oncol* 2007;5:84.
- 69 Kopp S, Warnke E, Wehland M, Aleshcheva G, Magnusson NE, Hemmersbach R, Juhl Corydon T, Bauer J, Infanger M, Grimm D: Mechanisms of three-dimensional growth of thyroid cells during long-term simulated microgravity. *Sci Rep* 2015;5:16691.
- 70 Gershovich YG, Buravkova LB: Effects of microgravity simulation on the production of interleukins in culture of human mesenchymal stromal cells. *Hum Physiol* 2011;37:860-865.
- 71 Li A, Dubey S, Varney ML, Dave BJ, Singh RK: IL-8 directly enhanced endothelial cell survival, proliferation, and matrix metalloproteinases production and regulated angiogenesis. *J Immunol* 2003;170:3369-3376.
- 72 Yu H, Huang X, Ma Y, Gao M, Wang O, Gao T, Shen Y, Liu X: Interleukin-8 Regulates Endothelial Permeability by Down-regulation of Tight Junction but not Dependent on Integrins Induced Focal Adhesions. *Int J Biol Sci* 2013;9:966-979.
- 73 Li L, Dong M, Wang X-G: The Implication and Significance of Beta 2 Microglobulin: A Conservative Multifunctional Regulator. *Chin Med J* 2016;129:448-455.
- 74 Khodarev NN, Park JO, Yu J, Gupta N, Nodzinski E, Roizman B, Weichselbaum RR: Dose-dependent and independent temporal patterns of gene responses to ionizing radiation in normal and tumor cells and tumor xenografts. *Proc Natl Acad Sci U S A* 2001;98:12665-12670.
- 75 Rogers JT: Ferritin translation by interleukin-1 and interleukin-6: the role of sequences upstream of the start codons of the heavy and light subunit genes. *Blood* 1996;87:2525-2537.
- 76 Ma X, Pietsch J, Wehland M, Schulz H, Saar K, Hübner N, Bauer J, Braun M, Schwarzwälder A, Segerer J, Birlem M, Horn A, Hemmersbach R, Waßer K, Grosse J, Infanger M, Grimm D: Differential gene expression profile and altered cytokine secretion of thyroid cancer cells in space. *FASEB J* 2014;28:813-835.